

CHENYE DUAN<sup>1</sup>, CHAO ZHANG<sup>1</sup>, RENHUI CHENG<sup>1</sup>,  
XIN LI<sup>2</sup>, XINGLONG WANG<sup>2</sup>

### PRESSURE RELIEF GAS DRAINAGE IN A FULLY MECHANISED MINING FACE BASED ON THE COMPREHENSIVE DETERMINATION OF 'THREE ZONES' DEVELOPMENT HEIGHT

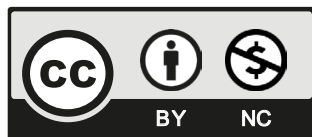
The gas emission from the goaf generates gas in the upper corner of the working face, and the return airflow exceeds safe limits. The identification of the reasonable level of the high-long borehole is the key factor to ensure the effectiveness of its extraction. On-site test at the 2308 working face of Licun Coal Industry of Lu'an Chemical Industry Group, the development of coal overlying strata fracture was studied through derivation of theoretical and empirical formulae, physical similarity experiment, and UDEC numerical simulation: this was then combined with in-situ microseismic monitoring to obtain the distribution characteristics of mining overburden "falling zone" and "overbreak zone" under the actual working conditions, and accurately design the high-level long borehole end hole layer. The results show that the height of the falling zone is 17.5 m to 20.5 m, and the overbreak zone is 43.5 m to 49.5 m. When the hole position is between 25 m and 30 m in the middle and lower part of the overbreak zone, the flow and concentration of gas extracted by drilling are high, and the pure amount of gas extracted by a single hole is increased by 53% (on average). The investigation of pressure relief gas extraction shows that throughout the mining period, the average gas concentration in the return airway is maintained below 0.36%, and the average gas concentration in the upper corner is kept within 0.48% (effective gas control). The research proves the rationality of the arrangement of the high-level long borehole horizon in the working face and provides a reference for the design of the borehole horizon in the future gas drainage and control in the goaf.

**Keywords:** Gas emission in goaf; mining overburden fracture; microseismic monitoring; high-long drilling; pressure relief gas extraction

<sup>1</sup> XI'AN UNIVERSITY OF SCIENCE AND TECHNOLOGY, CHINA

<sup>2</sup> SICHUAN UNIVERSITY, CHINA

\* Corresponding author: 13203456125@163.com



© 2024. The Author(s). This is an open-access article distributed under the terms of the Creative Commons Attribution-NonCommercial License (CC BY-NC 4.0, <https://creativecommons.org/licenses/by-nc/4.0/deed.en>) which permits the use, redistribution of the material in any medium or format, transforming and building upon the material, provided that the article is properly cited, the use is non-commercial, and no modifications or adaptations are made.

## 1. Introduction

Gas exceedance in the goaf and upper corner is the main reason restricting the development of coal mines [1,2]. To solve the problem of gas emission in the goaf during the mining of the working face, several mines in the Lu'an Mining Area, including Licun Coal Mine, have explored the high-level drilling gas control technique [3]. As a pressure relief gas extraction technology, high-level long drilling has been widely used because of its relatively low cost, flexible construction, and ability to solve the problem of gas exceedance in the upper corner and air return roadway [4,5]. The determination of the reasonable layer of the borehole is the key factor to ensure the effectiveness of the extraction [6-8]. When the borehole layer is arranged at a low level, highly affected by working face mining, and the borehole is easily damaged, it is not suitable for long-term stable gas extraction [9,10]. When the drilling horizon is high, cracks in the layout area are not developed, and the gas cannot migrate to the drilling horizon, resulting in significant extraction resistance and poor gas extraction effect [11-13]. Therefore, the optimisation and arranging of high-level long boreholes to achieve accurate gas extraction is one of the main problems facing engineers responsible for gas control.

Scholars have long investigated the fracture of overburden during coal mining and provided valuable theoretical and scientific bases for the development of overburden mining fractures. Qian et al. [14] and Xu et al. [15] studied the mining of working faces based on physical similarity experiment and numerical simulation experiment, systematically obtaining two processes of fracture development, and proposed the 'O-ring' theory of fracture development. Based on numerical modelling of the overburden, Gao et al. [16] analysed and determined the failure of overlying rock and the trend in surface movement. Based on the study of stress distribution in a full mechanisation caving face, Xie et al. [17] conducted in-depth exploration through numerical simulation and laboratory-similar material simulation and proposed the macro-scale stress-shell theory. Based on fractal theory, Li et al. [18]. And Wang et al. [19] studied the development of mining-induced fractures. The results showed that the middle and high-angle transition zone of fracture development is the critical area of gas extraction, and the extraction effect in this area is the strongest. Song et al. [20] used fractal theory to quantify the evolution of overlying strata cracks during and after mining. Liu et al. [21] used a comprehensive research method to study the development height of the water-conducting overbreak zone of the roof in fully mechanised caving mining of shallow and extra-thick coal seams. Taking the Lu'an mining area as the experimental background, Zhang et al. [22] used a fruit fly algorithm and a similar simulation experiment to study the development height of the overbreak zone in a fully mechanised mining face.

It is evident from the literature that the evolution of mining overburden cracks has achieved crucial research results after long-term development. In the process of mine gas extraction, the basic parameters of high-level boreholes are mostly determined based on theoretical formulae and experience, and it remains rare to combine theoretical guidance with actual overburden fissure development trends. In deep coal seam mining, the overburden strata are more complex, and this problem is more prominent, therefore, comprehensive laboratory simulation and in-situ testing to study the development of overburden fracture and determine the layout parameters of high-level boreholes are the preferred direction of development of high-level borehole pressure relief gas extraction, which can solution gas overrun in goaf and upper corner in a more efficient, rational manner.

In the present work, the 2308 working face of the Licun Coal Mine of Lu'an Chemical Industry Group was used as a model. The distribution characteristics of 'two zones' (falling zone

and overbreak zone) of mining overburden under actual working conditions were obtained by combining theoretical formula derivation, numerical simulation, similar simulation experiments, and in-situ microseismic monitoring. The variations of mining stress, the development of three zones and the development of microseismic events were explored, and the final hole horizon of high-level fracture drilling was optimised to research the effect of pressure relief gas extraction.

## 2. Project profile

Taking the 2308 working face of Licun Coal Mine as the test site, the panel length of the working face is 778 m, the face width is 252 m, and the thickness of the coal seam is 4.2 to 5 m, with an average of 4.6 m. The coal seam roof was dominated by sandy mudstone, siltstone, and medium-grained sandstone, and the floor was dominated by fine-grained sandstone, followed by sandy mudstone. Details of the roof and floor of the coal seam are provided in Fig. 1.

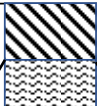



	Roof and floor	Rock type	Thickness (m)	Histogram	Lithological characteristics
Coal seam roof and floor situation	Main roof	Medium grained sandstone	5.8		Dark-grey, medium-thick layered, with muscovite debris and coal debris, partially fine sandstone, filled with calcite veins, containing many plant fossils.
	Immediate roof	Sandy mudstone, siltstone	14.9		Yellow, medium thick layer, loose mud, strong water absorption.
	Direct floor	Silt, sandy mudstone	3.7		Grey-black, medium thick layered, flat fracture, occasionally scattered pyrite.
	Base rock	fine-sandstone	7.4		Grey to dark-grey, medium-thick layer, mineral composition is mainly quartz, containing muscovite fragments and coal chips.

Fig. 1. Coal seam roof and floor data

## 3. Evolution of mining overburden overbreak zone

### 3.1. Empirical formula estimation

Through mechanical analysis and testing of the overlying strata on the 2308 working face of Licun Coal Mine (TABLE 1), the coal seam roof of the working face can be classified as being of the medium-hard roof type.

TABLE 1

Measured rock mechanics parameters of the overlying rock roof

	Compressive strength / MPa	Tensile strength / MPa	Deformation modulus / GPa	Elastic modulus / GPa
Main roof test results	36.11	1.56	9.43	11.75
Immediate roof test results	17.15	1.08	4.83	4.71

According to the empirical formula of ‘Buildings, water bodies, railway and main roadway coal pillar setting and coal mining regulations’, the development height of ‘two zones’ of overburden rock was calculated [23,24]. As shown in TABLES 1 and 2, the maximum development height of  $H_m$  in the falling zone is 15.42 to 20.43 m. The maximum development height of  $H_f$  in the overbreak zone is 36.37 to 47.57 m.

TABLE 2

Mining overburden height empirical formula

	Representative rock (medium hard)	Formula (m)
Falling zone ( $H_m$ )	Siltstone, argillaceous limestone, sandy mudstone, shale	$H_m = \frac{100 \sum M}{4.2 \sum M + 24} \pm 2.2$
Fissure zone ( $H_f$ )		$H_f = \frac{100 \sum M}{1.6 \sum M + 3.6} \pm 5.6$

## 3.2. Physical similar simulation experiment

### 3.2.1. Model construction

To simulate the actual overburdened geological conditions of the 2308 working face, a physical model (measuring 3000 mm × 200 mm × 1200 mm) was built (Fig. 2). For the construction of the physical model, mainly river sand, gypsum, calcium carbonate, and water (TABLE 3). The coal seam needs to be excavated every 20 minutes, and certain characteristics measured during each excavation. These include analysing the evolution and displacement of fractures, monitoring the settlement of each measuring point, and observing any separation fissures that occur after each periodic pressure.

In the boundary conditions, the bottom boundary of the model is fully constrained, and the two side boundaries and the front and rear boundaries of the model are one-way constrained boundaries. The thickness of the overlying rock layer over the simulated coal seam in the model is 116.3 m, and the remaining overlying rock layer is not laid down and loaded in the form of

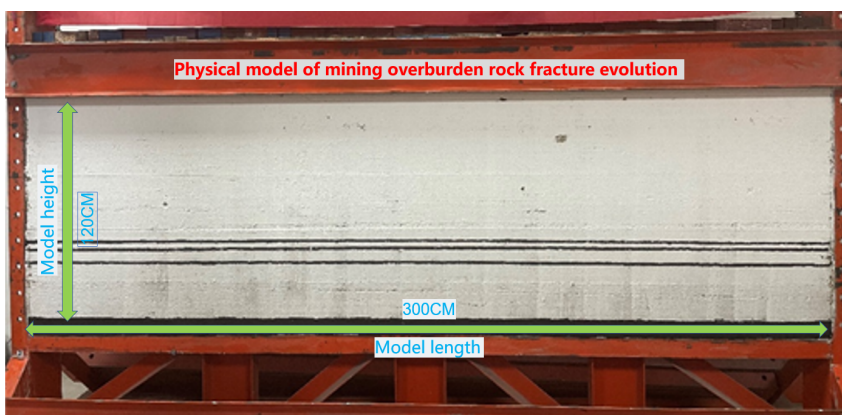


Fig. 2. The 3-m physical similar simulation shelf

a uniform load on the upper boundary of the model. After calculation, the mean distribution load loaded on the upper boundary of the model is 0.04 MPa.

- 1) Geometric similarity constant: the proportion of similarity in the geometric scale,  $\alpha_l = \frac{l_p}{l_m}$ , this experiment combined with laboratory conditions to choose the geometric similarity of 200.  
In the formula:  $\alpha_l$  is the geometric similarity constant,  $l_p$  is the size of the coal seam in the mine,  $l_m$  is the size of the test simulation.
- 2) Weight capacity similarity constant: the ratio of the density of the test prototype and the experimental model material,  $\alpha_\gamma = \frac{\gamma_p}{\gamma_m}$ , this experiment uses river sand as the skeleton and gypsum as the binder, the weight capacity similarity constant  $\alpha_\gamma$  takes the value of 1.5.  
In the formula:  $\gamma_p$  is the density of overburden rock material,  $\gamma_m$  is the density of rock material simulated by experiment.
- 3) Stress similarity constant: the similarity ratio of the overburden stress,  $\alpha_\sigma = \frac{\sigma_p}{\sigma_m}$ , the stress similarity ratio is the product of the geometric similarity ratio and the volumetric similarity ratio, so 300 is chosen.  
In the formula:  $\sigma_p$  is the stress of the prototype material,  $\sigma_m$  is the stress of the model material.
- 4) Strength similarity constant: According to the relationship between the strength constant and the stress similarity constant,  $\alpha_E = \alpha_\sigma = 150$  is obtained.
- 5) Poisson's ratio:  $\alpha_\mu = 0.25$ .

TABLE 3

Physical similarity simulation experiment ratio table

Serial number	Lithological characteristics	Sand (g)	Gypsum (g)	Calcium carbonate (g)	Coal ash (g)
1	Mudstone	8.667	0.375	0.583	/
2	Rock siltstone	8.583	0.250	0.833	/
3	Medium-grained sandstone	8.542	0.333	0.750	/
4	Fine-grained sandstone	8.563	0.438	0.646	/
5	Sandy mudstone	8.667	0.292	0.679	/
6	Coal	4.333	0.250	0.667	4.333

### 3.2.2. Results and analysis

The analysis of fracture evolution and fracture displacement of mining overburden rock is described here.

We excavated 80 mm from the 3 # coal to the model boundary at 200 mm (Corresponding to the actual size of 8 m, the following dimensions are actual dimensions) as a through-cut; when the working face is mined to 17 m, the immediate roof first collapses (Fig. 3); when the working face advances 24 m, the immediate roof periodically collapses (Fig. 4), and the main roof bends and sags to produce tensile fractures at both ends, but the fracture cracks do not penetrate the entire

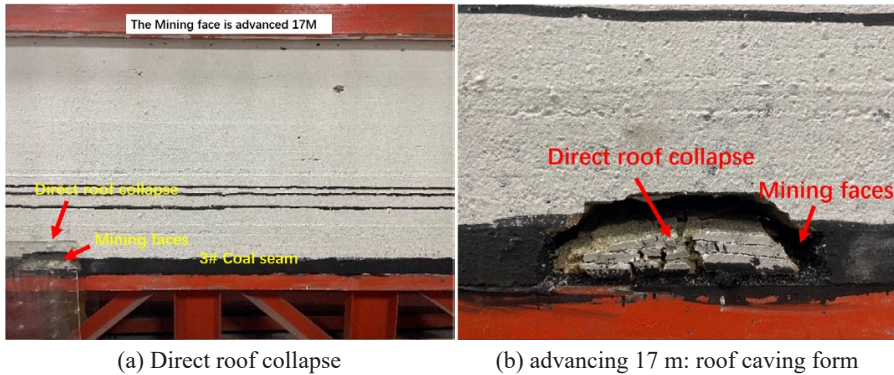


Fig. 3. After 17 m of face advance

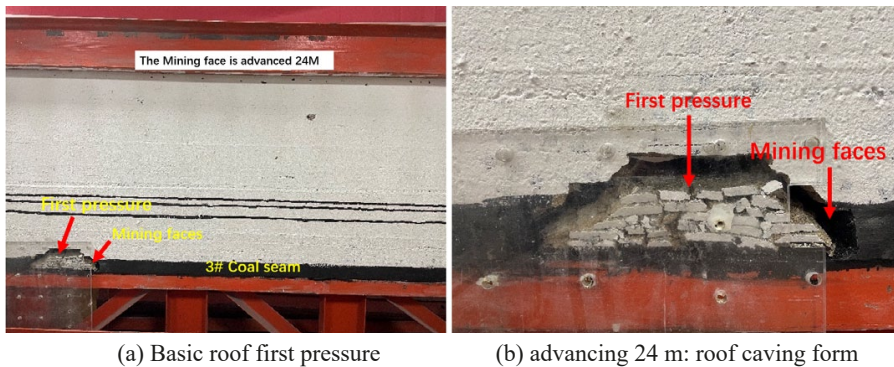


Fig. 4. After 24 m of face advance

rock layer, corresponding to the initial weighting of the main roof. In the process of advancing the working face from 24 m to 245 m, a total of 12 periodic weightings can occur (TABLE 4). When the 12<sup>th</sup> periodic weighting occurs at 209 m, the mass motion of the overlying strata in the goaf is quasi-stable, the bed separation cracks are no longer developed upward, the cavity is largely closed, and a relatively stable hinge structure is formed on the side of the working face. Most of the bed-separation cracks in the middle of the goaf have been closed.

When the working face is advancing, many oblique fracture fissures are formed on the side of the working face and the side of the cutting hole. In the early stage of advancement, there is an overbreak zone above the compaction zone. With the continuous advance of the working face, the cracks here are pressed down until they disappear. Finally, the central compaction zone is formed, and the final collapse form of the overbreak zone on both sides is formed. The overbreak zone on both sides is the main channel for gas transportation. The development of roof cracks can be expressed by crack distribution density and opening degree. The macroscopic crack opening of the rock mass to greater than 3 mm is deemed to be the development crack. According to the geometric similarity ratio of the model of 1:100, any model crack with a width exceeding 0.03 mm is a development crack, so the macroscopically visible cracks of the model can be regarded as a development crack. Herein, the height of the „two zones“ was analysed using the distribution



TABLE 4

Working face periodic weighting interval statistics

	Working face advancing length / m	Pressing step / m
First pressure	24	
The first cycle to pressure	35	11
The second cycle of pressure	52	17
The third cycle of pressure	71	19
The fourth cycle of pressure	89	18
The fifth cycle of pressure	104	15
The sixth cycle to pressure	119	15
The seventh cycle to pressure	133	14
The eighth cycle of pressure	150	17
The ninth cycle of pressure	164	14
The tenth cycle of pressure	179	15
The eleventh cycle to pressure	194	15
The twelfth cycle of pressure	209	15
The average periodic weighting step distance	15.4	

of macroscopically visible fractures. It is concluded that the height of the falling zone is 17.5 m. The height of the overbreak zone is 48.5 m.

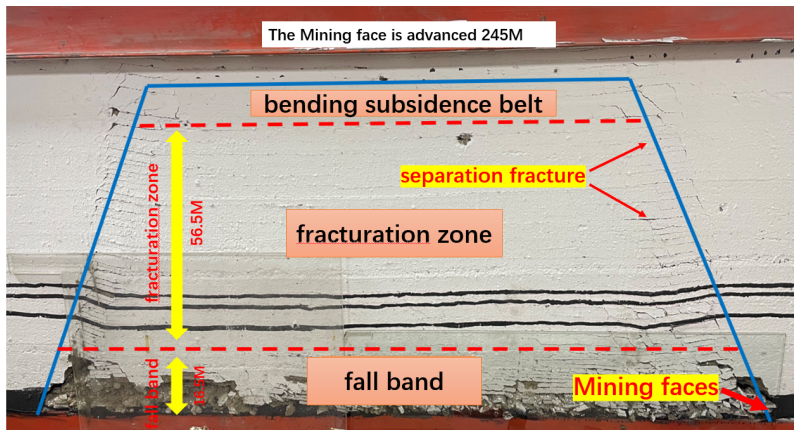


Fig. 5. Roof caving panorama after 245 m of face advance and three zone division

### 3.2.3. Movement and deformation

Experimental program: The coal seam cutting eye was set at 20 cm of the model boundary to protect the coal pillar. To monitor the collapse of overburden rock, ten measuring lines were set up on one side of the model. These lines were spaced 10 cm apart, with a single measuring point marked on each line at a 10 cm interval. The corresponding position of each measuring point was also noted and marked (Arrangement depicted in Fig. 6). The experimental coal seam mining

was completed several times, and the excavation was carried out once at an interval of 20 minutes. The characteristic parameters, such as the amount of subsidence of the measuring point that produces relative displacement and the off-seam fissure, are counted after each incoming pressure.

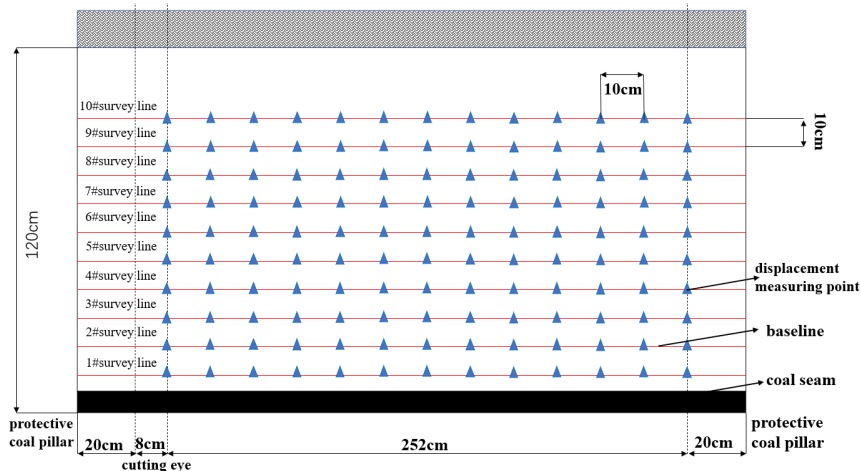
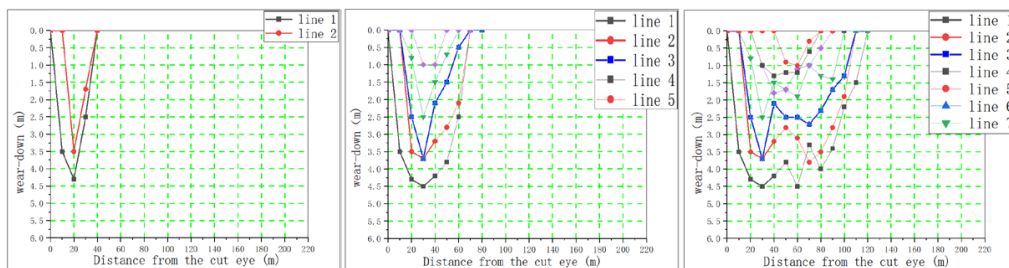
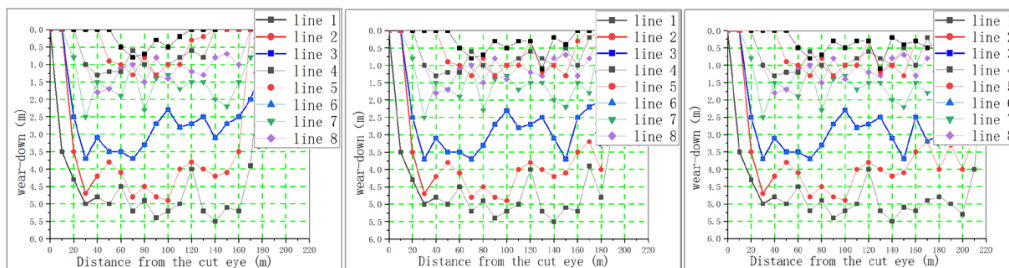


Fig. 6. Displacement measuring point layout

Fig. 7 shows the subsidence at each measuring point at different advances of the working face.



Working face advancing 35 m\71 m\104 m



Working face advancing 135 m\164 m\209 m

Fig. 7. Working face advancing measured subsidence



Fig. 7 shows that the subsidence of overlying strata from bottom to top is non-linear, and the moves are asymmetric. Due to the different strengths and thicknesses of rock strata and the development of strata and joints, the movement and caving steps of each rock stratum are also different. As the face advances, the height of the falling zone and the height over the fault zone continue to progress upwards, but this remains essentially unchanged as the face advances to 164 m. The height of the falling zone and the height over the fault zone continue to progress upwards as the face advances. The overlying strata (except the falling zone) undergo a continuous dynamic subsidence movement process during the mining operation, and the further from the coal seam, the more continuous the movement process and the shape of the movement curve is akin to the movement of the surface point. The closer to the coal seam, the more irregular the settling curve is. In general, the settling curve of the upper strata is akin to the settling curve of the surface. The maximum settling value of the overlying rock below the falling zone is located at the place of weighting, while the overlying rock above the falling zone is backwards, and its maximum subsidence is akin to that of the middle of the surrounding rock goaf.

### 3.3. Numerical simulation experiment research

#### 3.3.1. Establishment of numerical model

Based on an analysis of the actual conditions of 2308 working face in Licun Coal Mine, the discrete element program UDEC was used to simulate the evolution and stress distribution of overlying rock cracks under the influence of mining. When establishing the model, the parameters of the test mine are fully restored. The X axis is the mining direction of the working face, and the Y axis is the vertical plane of the coal seam. The height of the working face model is 120 m, and the length of the model is 400. There are 50 m long coal pillars on both sides of the model. The number of grids is 1897 430, the number of nodes is 3348 130, the block in the model is Mohr-Coulomb model, and the contact surface is Coulomb slip model. The displacement constraints were fixed around the perimeter and bottom edge of the model, and 12.0 MPa vertical stress was applied on the top edge to simulate the weight of the overlying rock layer, and the lateral pressure coefficient was taken as 1.3. The main change in subsidence during mining is within the vertical space, and the actual excavation length of the coal seam is 300 m. The initial model is shown in Fig. 8.

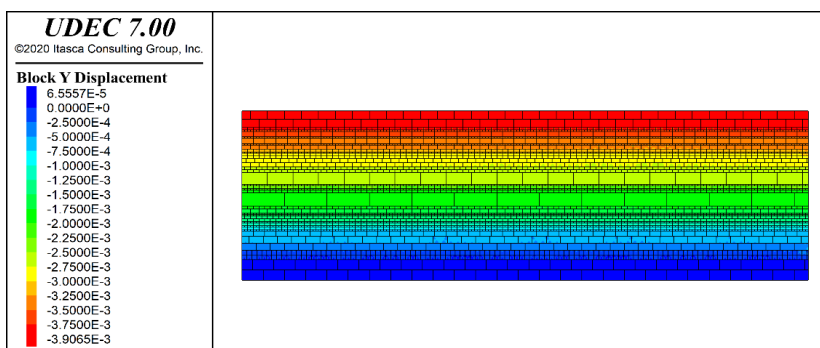


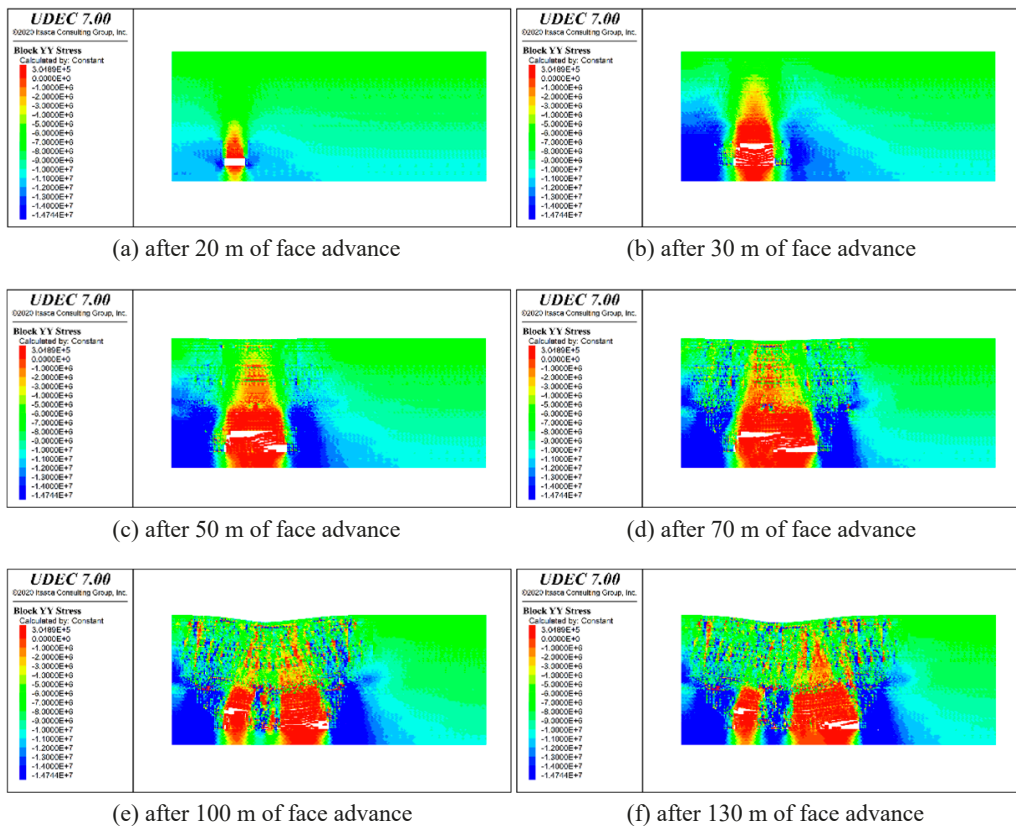
Fig. 8. UDEC numerical simulation model diagram

### 3.3.2. Analysis of effect

The total excavation length of the simulated working face is 300 m, which is divided into 10 excavations. The total length of each excavation is 20 m, 30 m, 50 m, 70 m, 100 m, 130 m, 160 m, 200 m, 240 m and 280 m respectively.

#### 1) Roof overburden rock breaking stress analysis of working face

Fig. 9 indicates that there are light green stress concentration areas in front of the working face at different stages, that is, the bearing stress increases in front of the working face. When the mining reaches 30 m, the basic roof will break for the first time, the advance support pressure will reach the maximum value, the maximum stress concentration will be 14.35 MPa, and the maximum stress in the stress-release area of the roof and floor will be 0.38 MPa; when the working face is mined to 160 m, the maximum stress concentration is 17.15 MPa, and the maximum stress in the stress-release area of the roof and floor is 0.34 MPa; when the working face advances to 200 m, the stress distribution in the stope changes to a significant extent, and different degrees of stress release occur in most strata. The maximum stress concentration is 19.15 MPa, and the maximum stress in the stress-release area of the roof and floor is 0.31 MPa; when the model is mined to 280 m, there is a compacted area in the goaf at 160 m behind the working face, and the stress as recovered to close to its original value.



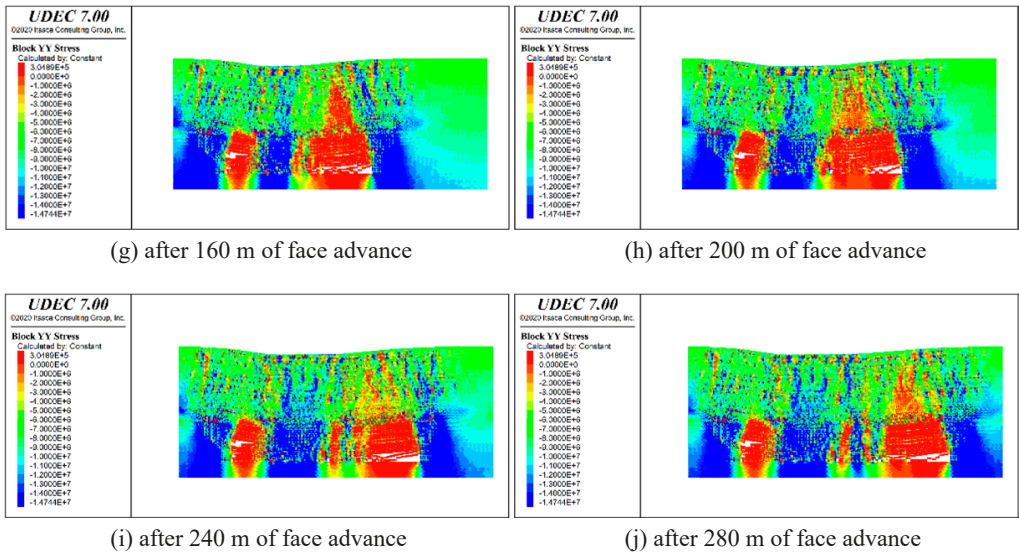


Fig. 9. Stress distribution diagram of overlying strata in goaf

2) Analysis of roof strata breaking displacement of working face

The fracture evolution process of overlying strata in the goaf is shown in Fig. 10.

As the working face is pushed forward to 30 m, the cantilever rock beam of the immediate roof bends and sinks under the effect of self-weight and the load of the main roof layer, resulting in fracture cracks, but the fracture cracks do not penetrate the whole rock layer, and the initial pressure is applied at this time. When the working face advances to 100 m, the direct roof of the coal seam collapses in a large area, and the collapsed rock will be compacted in the middle of the goaf. The rock falling on both sides of the goaf will expand slightly, and the overall height of the caving is close to 18.5 m. The cracks at the main roof then continue to develop upwards. When the working face is further excavated to 130 m, local cracks are generated at the cut hole and behind the mining face, and the rate of upward development of cracks above the goaf slows and decreases. The crack height is about 32 m, and the cracks begin to extend to the left and right sides of the rock mass. When the working face is excavated to 160 m, the immediate roof of the coal seam continues to be compacted in the middle of the goaf, the basic roof fracture develops upwards to about 43.5 m, and the break development pattern of the whole goaf is in the form on an inverted trapezoid. When the working face is excavated to 280 m, the fracture height on both sides of the goaf is higher than the overbreak zone height of the compacted area. The overall break develops forward with the direction of the coal seam, and the fracture is no longer developed upward. Finally, the height of the overbreak zone is maintained at between 32 m and 43.5 m. The rock strata above the overbreak zone produce normal bending under the action of self-weight, and the rock mass maintains the original integrity and is not as liable to collapse, forming a curved subsidence zone. According to the above analysis, the height of the falling zone is 18.5 m, and the height of the overbreak zone is 43.5 m.

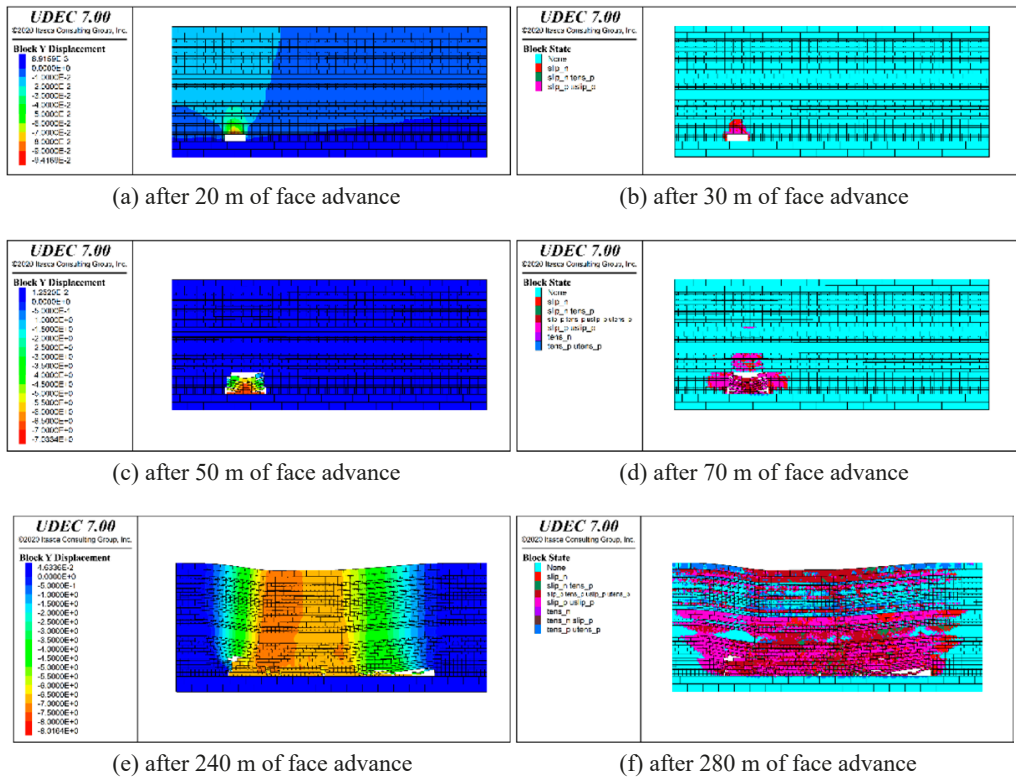


Fig. 10. Fracture evolution diagram of overlying strata in goaf

### 3.4. In-situ microseismic monitoring

#### 3.4.1. Establishment of a microseismic system

Based on the previous theoretical analysis, numerical simulation and similar simulation, the microseismic monitoring system was used to analyse the changes in the movement of the roof overburden and breakage during the back mining process of the 2308 working face and on-site measurements were carried out. Sensors were arranged on either side of the working face, and two sensors were connected to a datalogger. Sensors are arranged approximately 30 m in front of the work surface, with a distance of 15 metres between adjacent sensors (Fig. 11).

#### 3.4.2. Analysis of monitoring findings

By monitoring the distribution and distribution characteristics of microseismic events in different time periods, the spatial distribution pattern of microseismic events in the monitoring period is summarised.

Fig. 12 shows the statistical results of the distribution range of microseismic events in the vertical direction of the working face in different monitoring periods. From the broken line diagram, it can be seen that the upper bound of the distribution of microseismic events above the

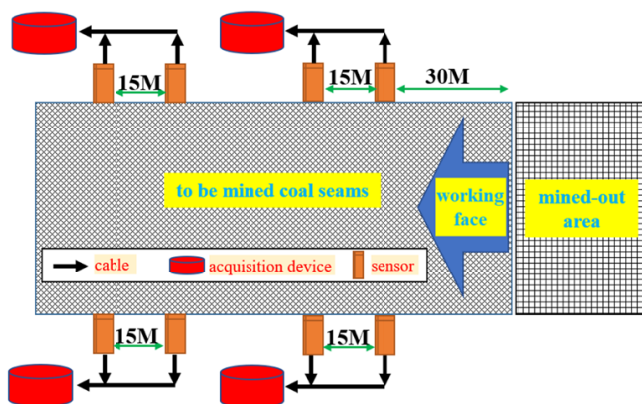


Fig. 11. Plan of the microseismic monitoring system

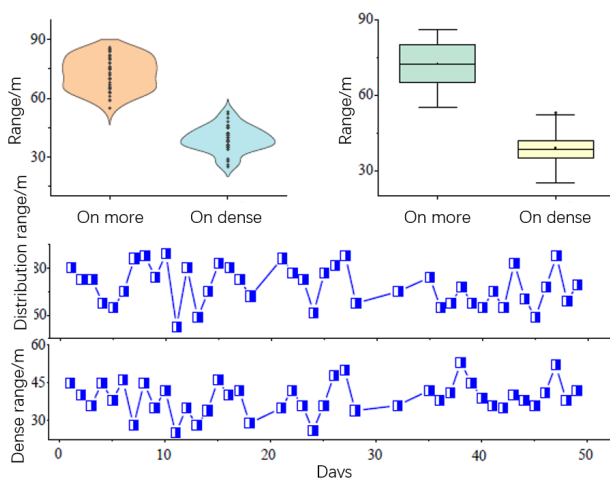


Fig. 12. Longitudinal distribution of microseismic event concentration range

working face is 55~86 m, and the upper boundary of the dense distribution of microseismic events is 25~53 m. From the violin and box diagrams, the upper boundary of the area with more distribution above the top is above 60 m, which is higher than the position of the upper boundary of the area with a dense event distribution. From the violin diagram, the upper boundary distribution of more microseismic event distribution above the working face is more concentrated (in the range of 61~85 m). The violin diagram shows a flat state, and the upper boundary of the microseismic event dense area above the working face is mostly within 29~50 m. The box diagram shows that the upper and lower quartile distances of the upper boundary of the dense area above are 35 m and 42 m respectively, with a median of 38 m. The upper and lower quartile positions of the upper boundary of the more active areas above are 65 m and 81 m respectively, with a median of 73 m. According to the comprehensive monitoring data, the height of the overbreak zone is 42.5~49.5 m, and the falling zone is 15.5~20.5 m.

### 3.5. Comprehensive determination of ‘two zones’ development height

Based on the derivation of the aforementioned empirical formula, numerical simulation, physical modelling, and in-situ microseismic monitoring experiment, It can be concluded that the development height of the “two zones” of the overlying strata in 2308 working face of the Licun Coal Industry (TABLE 5, wherein the upper limit is taken as the calculated result).

TABLE 5

The 2308 working face ‘two zones’ height determination

Assessment	Empirical formula	Analogue simulation	Numerical simulation	Microseismic monitoring	Comprehensive range
Height of falling zone (m)	20.4	17.5	18.5	20.5	17.5~20.5
Overbreak zone height (m)	47.6	48.5	43.5	49.5	43.5~49.5

Based on the data on the “two zones” development height of the 2308 working face in Licun Coal Mine, the difference in the development height of the falling zone is 17.14%, and the difference in the development height of the overbreak zone is 13.79%. Therefore, the theoretical study of the mining overburden fissure in the 2308 working face of the Licun coal mine compares with the measured data on-site, and the two are in good agreement.

## 4. *In-situ* testing

### 4.1. Layout and design of high-fracture drill holes

When arranging high-level boreholes, it is crucial to consider the number, size, and drainage capacity of the boreholes. Additionally, gas control in the local area of the upper corner and gas emission control in the entire goaf of the working face should be taken into account. In the range of 5 to 35 m near the return air roadway, the high and low layers of boreholes should be accurately arranged at different positions to achieve precise control of the gas concentration and flow from the top of the falling zone to the middle and lower part of the overbreak zone (at the vertical layer from 25 to 30 m). The borehole diameter used in this study is 203 mm, and seven boreholes are designed and constructed.

The parameters of the high-level long borehole arrangement are shown in TABLE 6, of which Boreholes 1 to 4 are low-level extraction boreholes; Boreholes 5 to 7 are high-level extraction holes arranged in the middle and lower parts of the fractured zone of the overlying strata, as shown in Fig. 13.

### 4.2. Effect investigation

Fig. 14 allows a comparison of gas extraction effects of different hole heights in high-level long boreholes.

Based on the results of on-site monitoring, the average value of gas extraction concentration of boreholes at a height of 12-18 m from the roof of the coal seam is 8.15%, and the extraction



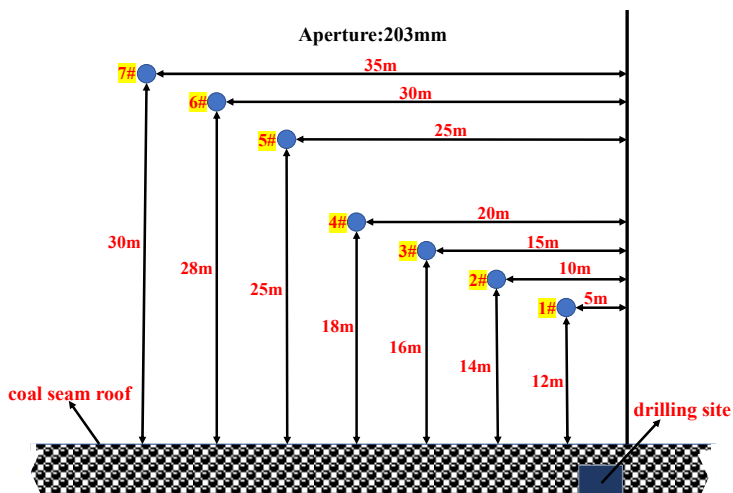


Fig. 13. Cross-section hole pattern

TABLE 6

Design parameters of high-level pressure relief borehole in kilometer drilling field

Hole number	Opening azimuth (°)	Opening angle (°)	Aperture (mm)	Hole depth (m)	Inside the return airway (m)	Distance from coal seam roof (m)
1	179.7	0.9	203	345	5	12
2	180.4	3.2		345	10	14
3	175.5	4.0		345	15	16
4	173.4	2.8		345	20	18
5	170.3	9.2		348	25	25
6	169.0	7.0		348	30	28
7	163.9	6.2		348	35	30

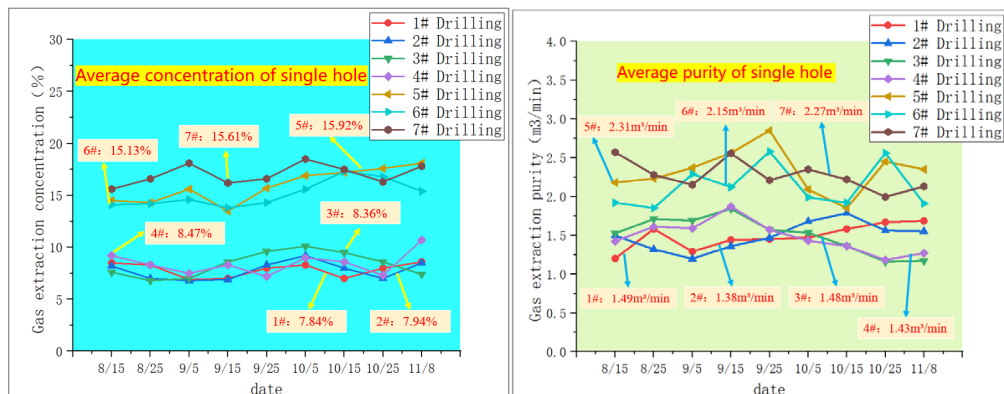


Fig. 14. Comparison of extraction concentration and pure quantity at different hole heights

concentration range varies from 6.5% to 10.7%. The average value of gas extraction quantity is  $1.45 \text{ m}^3/\text{min}$ , and the extraction quantity varies from  $1.19 \text{ m}^3/\text{min}$  to  $1.87 \text{ m}^3/\text{min}$ . The average value of gas extraction concentration of boreholes at a height of 25-30 m from the roof of the coal seam is 15.15%, the average value of gas extraction quantity is  $2.24 \text{ m}^3/\text{min}$ , and the range of gas extraction purities is  $1.85 \text{ m}^3/\text{min}$  to  $2.58 \text{ m}^3/\text{min}$ . The average gas extraction amount of a single hole is increased by 53%, and the gas extraction effect is significant, effectively reducing gas emissions in the goaf.

In summary, when the hole position is arranged within the range of 25 to 30 m in the middle and lower part of the overbreak zone, the flow and concentration of the gas extracted by the borehole are high, which proves that the arrangement of the high-level long borehole horizon in the working face is reasonable and correct. This also shows the feasibility of using the combination of empirical formula, UDEC numerical simulation, laboratory similar simulation, and in-situ microseismic monitoring to simulate the development of the overlying strata with its 'two zones' on the mining face. The drill holes are arranged in the position of 12 m~18 m in the fallout zone, although the concentration of the drill holes is slightly reduced, the mixed flow rate of the extraction is significant, and the gas concentration in the upper corner has a very good control effect, and the effect of the gas management in the upper corner is obvious. During the whole mining period, the average gas monitoring concentration in the return airway is maintained at below 0.36%, and the average gas concentration in the upper corner is kept within 0.48%, which meets the requirements for safe mining operations, therefore, the layout idea of large-diameter high-level boreholes in the goaf with consideration of gas control in the upper corner is reasonable, which also provides a reference for the design of borehole layers in gas extraction and control in the goaf in the future.

## 5. Conclusion

Through research, the following conclusions can be drawn:

- 1) Based on the laboratory simulation and in-situ testing, the development height of the overlying strata falling zone in the 2308 working face of Licun Coal Mine is 17.5 to 20.5 m, and the difference is 13.79%. The development height of the overbreak zone is 43.5-49.5 m, and the difference is 13.79%. The results are consistent and provide a reference for layer selection in high-level fracture drilling;
- 2) According to the results obtained, high and low-level boreholes are arranged at different positions, within the range of 5 to 35 m near the return airway. The extraction borehole diameter is 203 mm, the depth of the borehole is 345 m, and seven boreholes are designed and constructed. The results show that the flow and concentration of gas extracted by high-level drainage holes arranged in the middle and lower parts of the overbreak zone of the overlying strata (within 25-30 m in the vertical layer) are high, indicating that it is feasible to use the comprehensive judgement method to simulate the development of the 'two zones' of the overlying strata on the fully mechanised mining face;
- 3) The average gas concentration in the return alley is maintained below 0.36%, the average gas concentration in the upper corner is controlled at 0.48% or less, and the pure amount of single-hole gas extraction is increased by 53% (on average). A reasonable and correct method to judge the development height of the "two zones" of the mining overburden in

the 2308 working face and to design the horizon of the high-level borehole is proposed, which can provide an efficient and reasonable way to solve the problem of gas overrun in the goaf and upper corner.

## Reference

- [1] W. Tang, C. Zhai, J.Z. Xu, Y. Sun, Y.Z. Cong, Y.F. Zheng, The influence of borehole arrangement of soundless cracking demolition agents(SCDAs) on weakening the hard rock [J]. *Int. J. Min. Sci. Technol.* **31** (02), 197-207 (2021). DOI: <https://doi.org/10.1016/j.ijmst.2021.01.005>
- [2] J. Krawczyk, A preliminary study on selected methods of modeling the effect of shearer operation on methane propagation and ventilation at longwalls [J]. *Int. J. Min. Sci. Technol.*, **30** (05), 675-682 (2020). DOI: <https://doi.org/10.1016/j.ijmst.2020.04.007>
- [3] M.C. He, Q. Wang, Q.Y. Wu, Innovation and future of mining rock mechanics [J]. *J. Rock Mech. Geotech. Eng.* **13** (01), 1-21 (2021). DOI: <https://doi.org/10.1016/j.jrmge.2020.11.005>
- [4] Y.Y. Lu, Y.K. Zhang, J.R. Tang, Q. Yao, Switching mechanism and optimisation research on a pressure-attitude adaptive adjusting coal seam water jet slotter [J]. *Int. J. Min. Sci. Technol.* **32** (06), 1167-1179 (2022). DOI: <https://doi.org/10.1016/j.ijmst.2022.09.005>
- [5] L.Y. Shu, L. Yuan, Q.X. Li, W.T. Xue, N.N. Zhu, Z.S. Liu, Response characteristics of gas pressure under simultaneous static and dynamic load: Implication for coal and gas outburst mechanism [J]. *Int. J. Min. Sci. Technol.* **33** (02), 155-171 (2023). DOI: <https://doi.org/10.1016/j.ijmst.2022.11.005>
- [6] Q.L. Zou, Z.H. Chen, Y.P. Liang, W.J. Xu, P.R. Wen, B.C. Zhang, H. Liu, F.J. Kong, Evaluation and intelligent deployment of coal and coalbed methane coupling coordinated exploitation based on Bayesian network and cuckoo search [J]. *Int. J. Min. Sci. Technol.* **32** (06), 1315-1328 (2022). DOI: <https://doi.org/10.1016/j.ijmst.2022.11.002>
- [7] D.Y. Fan, X.S. Liu, Y.L. Tan, X.B. Li, P. Lkhamsuren, Instability energy mechanism of super-large section crossing chambers in deep coal mines [J]. *Int. J. Min. Sci. Technol.* **32** (05), 1075-1086 (2022). DOI: <https://doi.org/10.1016/j.ijmst.2022.06.008>
- [8] H.H. Fang, C.S. Zheng, N. Qi, H.J. Xu, H.H. Liu, Y.H. Huang, Q. Wei, X.W. Hou, L. Li, S.L. Song, Coupling mechanism of THM fields and SLG phases during the gas extraction process and its application in numerical analysis of gas occurrence regularity and effective extraction radius [J]. *Pet. Sci.* **19** (03), 990-1006 (2022). DOI: <https://doi.org/10.1016/j.petsci.2022.01.020>
- [9] S.K. Singh, B.P. Banerjee, S. Raval, A review of laser scanning for geological and geotechnical applications in underground mining [J]. *Int. J. Min. Sci. Technol.* **33** (02), 133-154 (2023). DOI: <https://doi.org/10.1016/j.ijmst.2022.09.022>
- [10] M.Z. Gao, H.M. Li, Y. Zhao, Y.T. Liu, W.Q. Zhou, L.M. Li, J. Xie, J. Deng, Mechanism of micro-wetting of highly hydrophobic coal dust in underground mining and new wetting agent development [J]. *Int. J. Min. Sci. Technol.* **33** (01), 31-46 (2023). DOI: <https://doi.org/10.1016/j.ijmst.2022.11.003>
- [11] X.Q. He, C. Zhou, D.Z. Song, Z.L. Li, A.Y. Cao, S.Q. He, M. Khan, Mechanism and monitoring and early warning technology for rockburst in coal mines [J]. *Int. J. Min. Met. Mater.* **28** (07), 1097-1111 (2021). DOI: <https://doi.org/10.1007/s12613-021-2267-5>
- [12] Z. Liu, X. Zhong, H. Ren, et al., Redevelopment of Fractures and Permeability Changes after Multi-Seam Mining of Shallow Closely Spaced Coal Seams [J]. *Archives of Mining Sciences* **64** (4), 671 (2019). DOI: <https://doi.org/10.24425/ams.2019.129376>
- [13] M. Mynarczuk, M. Skiba, An Approach to Detect Local Tectonic Dislocations in Coal Seams Based on Roughness Analysis [J]. *Archives of Mining Sciences* **67** (4), 743 (2022). DOI: <https://doi.org/10.24425/ams.2022.143685>
- [14] M.G. Qian, J.L. Xu, Coal mining and strata movement [J]. *Coal Journal* **44** (04), 973-984 (2019). DOI: <https://doi.org/10.13225/j.cnki.jccs.2019.0337>
- [15] M.G. Qian, J.L. Xu, Research on the 'O'-shaped circle characteristics of mining-induced fracture distribution in overlying strata [J]. *Coal Journal* (05), 20-23 (1998). DOI: <https://doi.org/10.13225/j.cnki.jccs.1998.05.004>

- [16] Y.F. Gao, W.P. Huang, G.L. Qu, B. Wang, X.H. Cui, Q.Z. Fan, Perturbation effect of rock rheology under uniaxial compression [J]. *J. Cent. South Univ.* **24** (07), 1684-1695 (2017). DOI: <https://doi.org/10.1007/s11771-017-3575-9>
- [17] G.X. Xie, J.Z. Li, L. Wang, Y.Z. Tang, Mechanical characteristics and time-space evolution of stress shell of surrounding rock in stope floor [J]. *Coal Journal* **43** (01), 52-61 (2018). DOI: <https://doi.org/10.13225/j.cnki.jccs.2017.0003>
- [18] H.Y. Li, W.H. Wang, Q.X. Qi, L. Zhang, Study on space-time evolution law of mining-induced fractures based on fractal theory [J]. *Coal Journal* **39** (06), 1023-1030 (2014). DOI: <https://doi.org/10.13225/j.cnki.jccs.2013.0027>
- [19] W.H. Wang, Research on seepage law of mining overburden fracture based on fractal theory [J]. *Coal Technology* **34** (09), 208-211 (2015). DOI: <https://doi.org/10.13301/j.cnki.ct.2015.09.080>
- [20] B.X. Song, L. Chen, F.W. Zhang, L. Chen, H.Y. Li, Fractal theory to study the evolution of mining fissures [J]. *Engineering Investigation* **45** (01), 1-6 (2017).
- [21] Z.X. Liu, S.N. Dong, D.W. Jin, X.M. Guo, Y.F. Liu, J. Yang, K. Guo, H.B. Shang, Formation mechanism and prevention of underground debris flow induced by support crushing and roof cutting in deep buried stope [J]. *Coal Journal* **44** (11), 3515-3528 (2019). DOI: <https://doi.org/10.13225/j.cnki.jccs.2019.0366>
- [22] B.A. Zhang, J.Y. Li, Y. Lu, C.H. Liu, Comparative analysis of prediction methods for height of water flowing fractured zone in overlying strata of goaf [J]. *Chinese Journal of Geological Disasters and Prevention* **27** (02), 132-136 (2016). DOI: <https://doi.org/10.16031/j.cnki.issn.1003-8035.2016.02.21>
- [23] H.Y. Dai, P. Li, N. Marzhan, Y.G. Yan, C.L. Yuan, T. Serik, J.T. Guo, Y. Zhakypbek, K. Seituly, Subsidence control method by inversely-inclined slicing and upward mining for ultra-thick steep seams [J]. *Int. J. Min. Sci. Technol.* **32** (01), 103-112 (2022). DOI: <https://doi.org/10.1016/j.ijmst.2021.10.003>
- [24] J.G. Ning, J. Wang, Y.L. Tan, Q. Xu, Mechanical mechanism of overlying strata breaking and development of fractured zone during close-distance coal seam group mining [J]. *Int. J. Min. Sci. Technol.* **30** (02), 207-215 (2020). DOI: <https://doi.org/10.1016/j.ijmst.2019.03.001>